CrystEngComm

Accepted Manuscript

ROYAL SOCIETY OF CHEMISTRY

www.rsc.org/crystengcomm

Supersaturation-induced hydrothermal formation of α-$CaSO_4 \cdot 0.5H_2O$ whiskers

S.C. Hou[a], J. Wang[a], T.Y. Xue[a], W.J. Zheng[b] and L. Xiang[a*]

[a] Department of Chemical Engineering, Tsinghua University, Beijing 100084, China

[b] School of Material and Mechanical Engineering, Beijing Technology and Business University, Beijing 100037, China

ABSTRACT: The supersaturation-induced hydrothermal formation of α-$CaSO_4 \cdot 0.5H_2O$ whiskers from $CaSO_4 \cdot 2H_2O$ precursor at 115-150°C was investigated in this paper. The experimental results indicated that the conversion processes were carried out via the dissolution-precipitation and homogeneous nucleation routes and connected with the critical supersaturation (abbreviated as S_{crit}, $\ln S_{crit} = a(\gamma/T)^{3/2}$) of the system. In the temperature range of 115-150°C, α-$CaSO_4 \cdot 0.5H_2O$ whiskers with a length of 200-500 μm and a diameter of 0.1-0.5 μm formed quickly within 2.0-5.0 minutes once the supersaturation (abbreviated as S) reached up to S_{crit}. The supersaturation-induced formation of α-$CaSO_4 \cdot 0.5H_2O$ consisted well with the first-order reaction model, and the corresponding activation energy (E_a) and the pre-exponent factor (A_0) were 161.7 kJ·mol^{-1} and 2.601×10^{21} h^{-1}, respectively.

KEY WORDS: α-$CaSO_4 \cdot 0.5H_2O$ whiskers, critical supersaturation, hydrothermal formation, dissolution-precipitation

INTRODUCTION

Hydrothermal synthesis is one of the widely used methods to prepare crystals with multiple applications, including zeolites[1], lithium iron phosphate cathodes[2], ZnO nanorods[3-7] and $CaSO_4 \cdot 0.5H_2O$ whiskers[8], etc., owing to the moderate conditions and the formation of the products with high crystallinity and little defects[9]. Two mechanisms (in situ transformation and dissolution-precipitation) are usually used to explain the hydrothermal formation of the crystals.

Supersaturation is one of the important factors that influence the morphology and the formation mechanisms of the crystals[10-12]. For example, PbS wires were produced on the quartz substrate via the vapor-liquid-solid (VLS) route at low supersaturation and via the bulk vapor-solid (VS) deposition at high supersaturation[11]. The growth of K_2SO_4 crystals in the presence of Cr(III) was suppressed at $S<8.0\times10^{-3}$, and promoted with the increase of the supersaturation if $S\geq8.0\times10^{-3}$ [12]. Crystal nuclei formed above the critical supersaturation (S_{crit}) and then grew to microscopic sizes[13]. The critical supersaturation for the growth of $BaSO_4$ and $SrSO_4$ crystals were 7.0 and 2.3, respectively, above which two-dimensional nucleation and growth occurred on (001) of the two crystals[10]. Alpha-lactose monohydrate (αLM) nuclei with tomahawk, triangular, pyramidal and needle-like shapes formed at the supersaturation of 0.97-1.62,

* Corresponding author. E-mail.xianglan@mail.tsinghua.edu.cn

1.62-2.34, 2.34-3.46 and 3.46-5.65, respectively[14].

Some work has been carried out to reveal the formation mechanisms and kinetics in aqueous system containing α-$CaSO_4 \cdot 0.5H_2O$ and/or $CaSO_4 \cdot 2H_2O$ [15-18]. It was reported that the conversion of α-$CaSO_4 \cdot 0.5H_2O$ to $CaSO_4 \cdot 2H_2O$ in water (20°C) was carried out via dissolution-precipitation route because $CaSO_4 \cdot 2H_2O$ was more thermodynamically stable than α-$CaSO_4 \cdot 0.5H_2O$ at room temperature[16], while the hydrothermal conversion (120-150°C) of $CaSO_4 \cdot 2H_2O$ to α-$CaSO_4 \cdot 0.5H_2O$ was happened via dissolution-precipitation since α-$CaSO_4 \cdot 0.5H_2O$ was more thermodynamically stable than $CaSO_4 \cdot 2H_2O$ at elevated temperature[8, 19-20]. The heterogeneous nucleation of $CaSO_4 \cdot 2H_2O$ in the presence of sand substrates was a second-order precipitation process[21], and the subsequent crystallization of $CaSO_4 \cdot 2H_2O$ in the temperature range of 15 - 45°C was controlled by the surface growth with an activation energy of 15.0 kcal·mol^{-1} [22]. Up to now little work concerned with the influence of supersaturation on hydrothermal formation of α-$CaSO_4 \cdot 0.5H_2O$ from $CaSO_4 \cdot 2H_2O$, which limited the controllable synthesis and optimization of α-$CaSO_4 \cdot 0.5H_2O$ whiskers.

The present work investigated the influence of supersaturation on the hydrothermal conversion of $CaSO_4 \cdot 2H_2O$ to α-$CaSO_4 \cdot 0.5H_2O$, focusing mainly on the influence of the critical supersaturation on the conversion kinetics and process mechanisms. The dissolution-precipitation mechanism was suggested and the homogeneous nucleation processes were studied in detail.

EXPERIMENTAL

Experimental procedure

AR $CaSO_4 \cdot 2H_2O$ with a purity of 99.0% was first sintered at 150°C for 6.0 h, then mixed with deionized water at room temperature to get the slurries containing 1.0-5.0 wt% $CaSO_4 \cdot 2H_2O$. The slurries were then treated at 115-150 °C for 30-120 min. After hydrothermal treatment, the samples were cooled down to 90-95°C in 5-10 minutes with cooling water, then the precipitates and the solutions were separated by filtration, the precipitates were dried at 90°C for 6.0 h and the solutions were gathered for chemical analyses.

Characterization

The morphology of the samples were detected with the field emission scanning electron microscopy (SEM, JSM 7401F, JEOL, Japan). The structures of the samples were identified by powder X-ray diffractometer (XRD, D8 advanced, Brucker, Germany) using Cu Kα radiation (λ=1.54178Å). The composition of the hydrothermal products was detected by the thermogravimetry (TG, NETZSCH STA 409C, Switzerland) under nitrogen atmosphere with a

heating rate of 10°C·min^{-1}. The concentrations of the total soluble Ca^{2+} and SO_4^{2-} in the solutions were detected by EDTA titration and $BaCrO_4$ spectrophotometric method, respectively.

RESULTS AND DISCUSSIONS

Formation of α-$CaSO_4$·0.5H_2O whiskers

Figure 1 shows the variation of the composition of the hydrothermal products with temperature and reaction time. The induction time needed for the formation of $CaSO_4$·0.5H_2O were 110 min at 115°C, 90 min at 120°C, 53 min at 135°C and 24.5 min at 150°C, respectively, indicating the decrease of the induction time with the increase of the temperature. $CaSO_4$·2H_2O was then converted to $CaSO_4$·0.5H_2O quickly and the time needed for the phase transformation were 5.0 min at 115°C, 5.0 min at 120°C, 2.0 min at 135°C and 2.0 min at 150°C, respectively, revealing the acceleration of the phase transformation with the increase of the temperature.

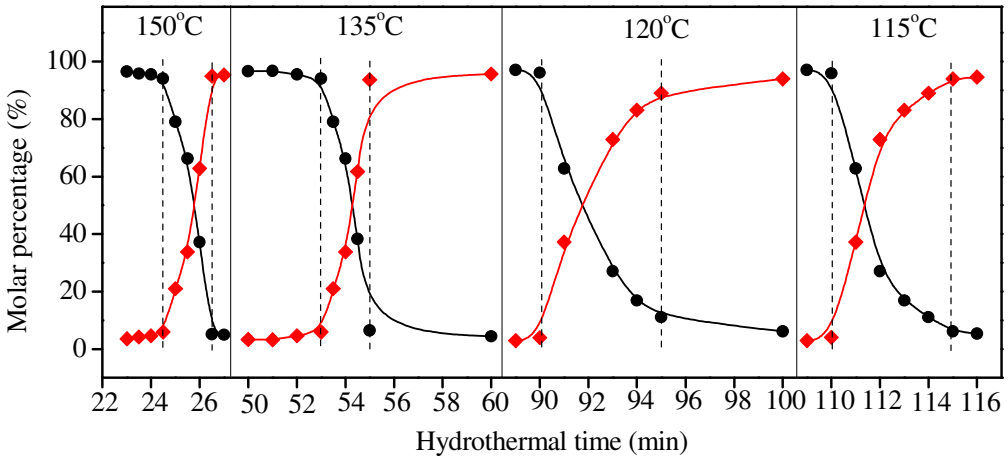

Figure 1 Variation of composition of hydrothermal products with temperature and reaction time

●-$CaSO_4$·2H_2O, ◆-α-$CaSO_4$·0.5H_2O.

Figure 2 shows the variation of the concentration of Ca^{2+} and SO_4^{2-} ($[Ca^{2+}]$ and $[SO_4^{2-}]$) with temperature and reaction time. The increase of temperature from 115°C to 150°C led to the decrease of $[Ca^{2+}]$ and $[SO_4^{2-}]$ due to the decrease of the solubility of $CaSO_4$·2H_2O and $CaSO_4$·0.5H_2O with the increase of temperature[15]. The initial increase of $[Ca^{2+}]$ and $[SO_4^{2-}]$with the increase of reaction time may be connected with the faster dissolution of $CaSO_4$·2H_2O than the precipitation of $CaSO_4$·0.5H_2O, and the subsequent decrease of $[Ca^{2+}]$ and $[SO_4^{2-}]$with the prolongation of reaction time should be attributed to the faster precipitation of $CaSO_4$·0.5H_2O than the dissolution of $CaSO_4$·2H_2O. The above work demonstrated the possible dissolution-precipitation mechanism for the fast transformation of $CaSO_4$·2H_2O

to $CaSO_4 \cdot 0.5H_2O$.

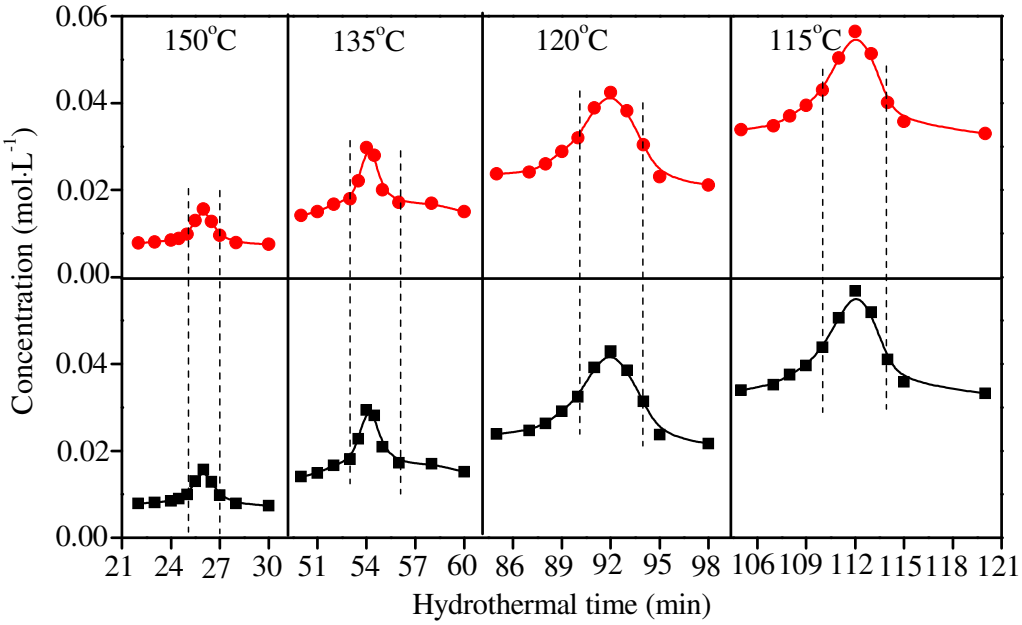

Figure 2 Variation of $[Ca^{2+}]$ and $[SO_4^{2-}]$ with temperature and reaction time

■: $[Ca^{2+}]$, ●: $[SO_4^{2-}]$.

Figure 3 and Figure 4 show the variation of the morphology and the XRD patterns of the hydrothermal products with temperature and time, respectively. After induction for 24.5-110 minutes in the temperature range of 115-150°C, the $CaSO_4 \cdot 2H_2O$ plates and rods were converted to the highly crystallized α-$CaSO_4 \cdot 0.5H_2O$ whiskers quickly (within 2.0-5.0 minutes). Before the occurrence of α-$CaSO_4 \cdot 0.5H_2O$, the products were composed of the $CaSO_4 \cdot 2H_2O$ which was consisted of the plates with a width of 4-5 μm and the rods with a diameter of 1-2 μm (Figure 3a, 3d, 3g, 3j, 4a, 4d, 4g and 4j). α-$CaSO_4 \cdot 0.5H_2O$ whiskers with a diameter of 0.1-0.5 μm and a length of 50-200 μm occurred and co-existed with the plate-like $CaSO_4 \cdot 2H_2O$ particles after 0.5-2.0 minutes of reaction (Figure 3b, 3e, 3h, 3k, 4b, 4e, 4h and 4k). The products were composed of α-$CaSO_4 \cdot 0.5H_2O$ whiskers with a diameter of 0.1-1.0 μm and a length of 100-400 μm after further reaction for 1.0-2.0 minutes (Figure 3c, 3f, 3i, 3l, 4c, 4f, 4i and 4l).

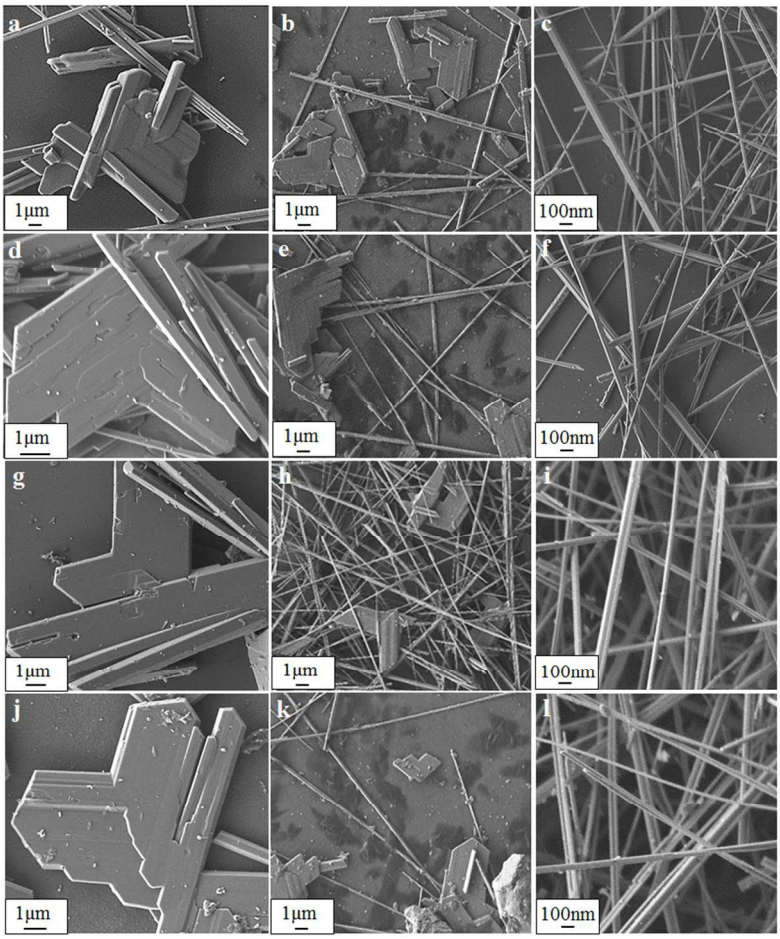

Figure 3 Variation of morphology of hydrothermal products with temperature and time

Temperatures (°C): a, b, c-115; d, e, f-120; g, h, i-135; j, k, l-150; time (min): a-108, b-110, c-112, d-90, e-91, f-93, g-53, h-54, i-55, j-24.5, k-25, l-26.

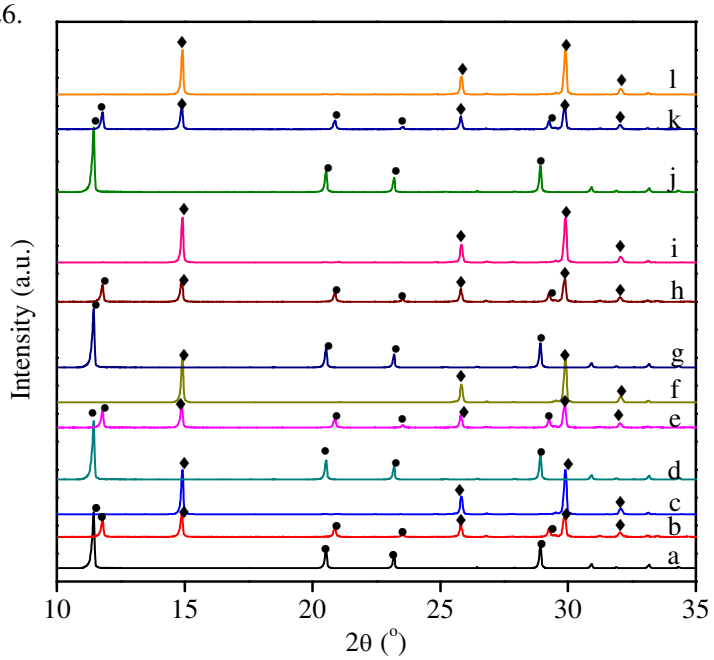

Figure 4 Variation of XRD patterns of hydrothermal products with temperature and time

Temperatures (°C): a, b, c-115; d, e, f-120; g, h, i-135; j, k, l-150; time (min): a-108, b-110, c-112, d-90, e-91, f-93, g-53, h-54, i-55, j-24.5, k-25, l-26; ●-$CaSO_4·2H_2O$, ◆-α-$CaSO_4·0.5H_2O$.

Supersaturation-induced fast conversion of $CaSO_4·2H_2O$ to $CaSO_4·0.5H_2O$

Figure 5 shows the variation of the supersaturation with temperatures and time, based on the calculated data shown in Figure 2. The supersaturation was defined as $S = \frac{[Ca^{2+}][SO_4^{2-}]}{K_{sp}}$, where $[Ca^{2+}]$ and $[SO_4^{2-}]$ were the concentrations of the Ca^{2+} an SO_4^{2-} in the solutions, and K_{sp} was calculated out by HSC Chemistry 7.0[22].

The variation of the supersaturation with reaction time was quite similar to those of $[Ca^{2+}]$ and $[SO_4^{2-}]$: increased firstly to a maximum point and then decreased to a low level. The critical supersaturations at which the fast transformation started were 209.4, 140.5, 81.3 and 46.7 at 115°C, 120°C, 135°C and 150°C, respectively.

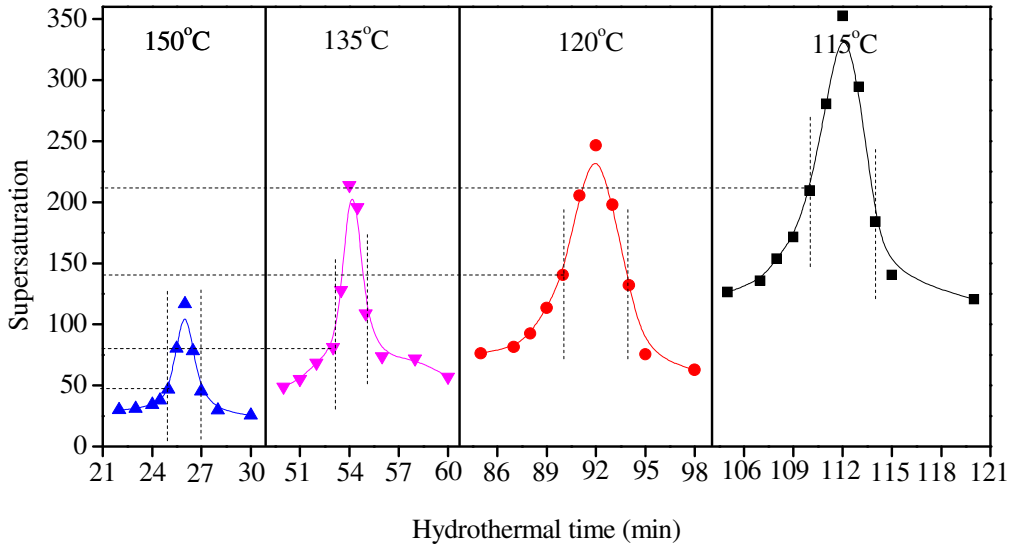

Figure 5 Variation of supersaturation with temperature and time

The critical supersaturation for the dissolution-precipitation and homogeneous nucleation process can be deduced from the classical nucleation theory[23]:

$$\Delta G = 4\pi r^2\gamma + \frac{4}{3}\pi r^3 \Delta G_v \quad (3.1)$$

$$J = A\exp(-\frac{\Delta G}{kT}) \quad (3.2)$$

$$\ln S = \frac{2\gamma v}{kTr} \quad (3.3)$$

where ΔG_v is the change of the free energy for the phase transformation per unit volume, γ is the interfacial tension, J is the nucleation rate, e.g. the number of nuclei formed per unit time per unit volume, k is the Boltzmann constant, A is the pre-exponential factor, S is the supersaturation of the solute, v is the molecular volume, r is the radium of the particles.

Then

$$\ln S_{crit}=a\left(\frac{\gamma}{T}\right)^{3/2} \tag{3.4}$$

where a is a constant

$$a=\left[\frac{16\pi v^2}{3k^3 \ln A}\right]^{1/2} \tag{3.5}$$

It is known from Equation (3.4) that $\ln S_{crit}$ should keep a linear relationship with $(\gamma/T)^{3/2}$.

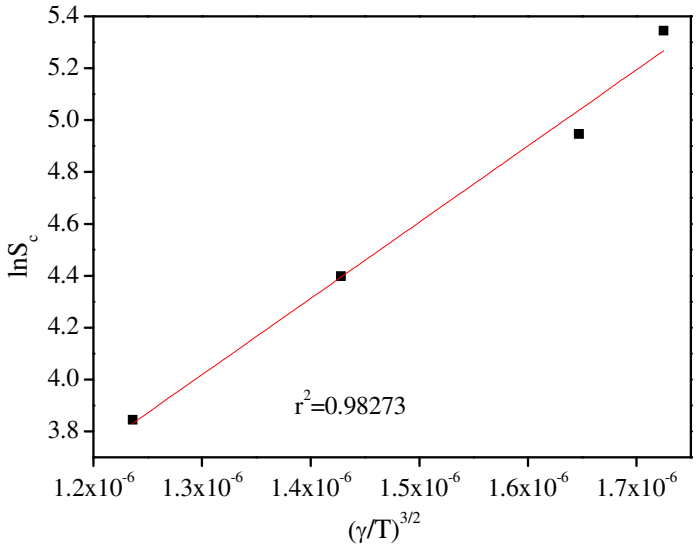

Figure 6 $\ln S_{crit}$ vs $(\gamma/T)^{3/2}$

Figure 6 shows the fitting results of $\ln S_{crit}$ vs $(\gamma/T)^{3/2}$. The linear relationship between $\ln S_{crit}$ and $(\gamma/T)^{3/2}$with a dependent coefficient of 0.98273 indicated that the fast conversion of $CaSO_4 \cdot 2H_2O$ to α-$CaSO_4 \cdot 0.5H_2O$ whiskers which was induced by the critical supersaturation was carried out via the dissolution-precipitation and homogeneous nucleation route.

Kinetics of the fast conversion process

The conversion process of $CaSO_4 \cdot 2H_2O$ to α-$CaSO_4 \cdot 0.5H_2O$ can be represented as

$$CaSO_4 \cdot 2H_2O(A) \xrightarrow{k} CaSO_4 \cdot 0.5H_2O(B) + 1.5H_2O \tag{4.1}$$

where A and B represents $CaSO_4 \cdot 2H_2O$ and α-$CaSO_4 \cdot 0.5H_2O$, respectively, k is the reaction constant.

Assuming reaction (4.1) to be a first-order reaction, then k can be expressed as

$$k = \frac{1}{t} \ln \frac{x_A}{x_{A0}} \tag{4.2}$$

where x_{A0} and x_A is the molar ratio of $CaSO_4 \cdot 2H_2O$ at 0 and t moment, respectively. x_A / x_{A0} can be figured out from the data in Figure 1.

Figure 7 shows the plots of $\ln(x_A / x_{A0})$ against reaction time. The linear relationship between $\ln(x_A / x_{A0})$ and the reaction time indicated that the fast conversion of $CaSO_4 \cdot 2H_2O$ to α-$CaSO_4 \cdot 0.5H_2O$ at different temperatures consisted well with the first-order reaction model. The increase of temperature from 115°C to 150°C led to the increase of the rate constant from 0.3622 min^{-1} to 1.6582 min^{-1}.

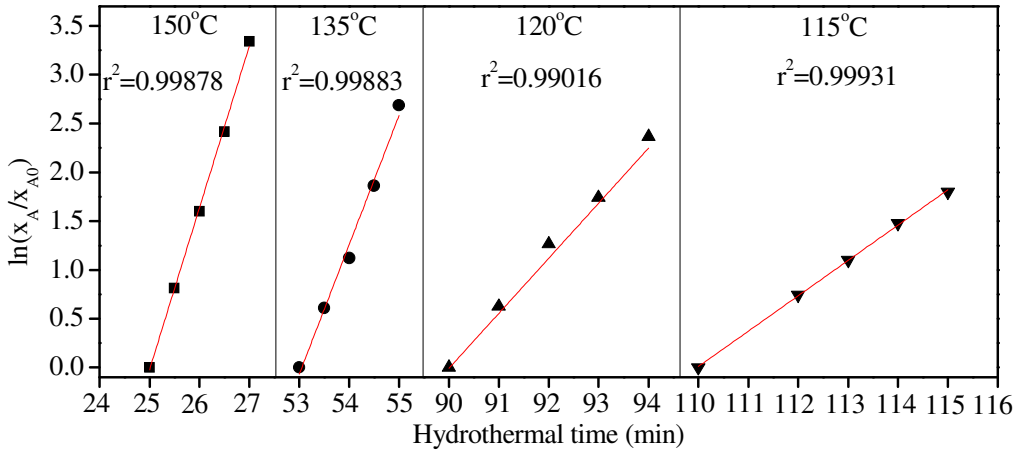

Figure 7 $\ln(x_A / x_{A0})$ vs reaction time

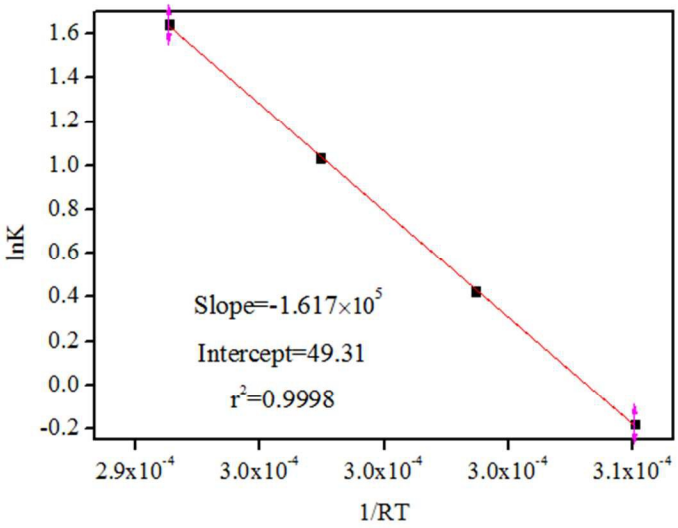

Figure 8 lnK vs 1/RT

Figure 8 shows the plots of lnK against 1/RT. The regression analyses of the slope and the intercept in Figure 8 indicated that the activation energy (E_a) and the pre-exponent factor (A_0) were 161.7 kJ·mol^{-1} and 2.601×10^{21} h^{-1}, respectively. The high E_a and A_0 indicated that the fast conversion of $CaSO_4·2H_2O$ to α-$CaSO_4·0.5H_2O$ was sensitive to both temperature and reaction time.

CONCLUSION

The quick hydrothermal conversion of $CaSO_4·2H_2O$ to α-$CaSO_4·0.5H_2O$ in the temperature range of 115-150°C was experimentally observed. The conversion processes were induced by the supersaturation and carried out via dissolution-precipitation and homogeneous nucleation routes. In the temperature range of 115-150°C, α-$CaSO_4·0.5H_2O$ whiskers with a length of 200-500 μm and a diameter of 0.1-0.5 μm formed quickly within 2.0-5.0 minutes once the solution supersaturation reached up to S_c. The formation rates of α-$CaSO_4·0.5H_2O$ consisted well with the first-order reaction model, and the activation energy (E_a) and the pre-exponent factor (A_0) were 161.7 kJ·mol^{-1} and 2.601×10^{21} h^{-1}, respectively.

TABLE OF CONTENT

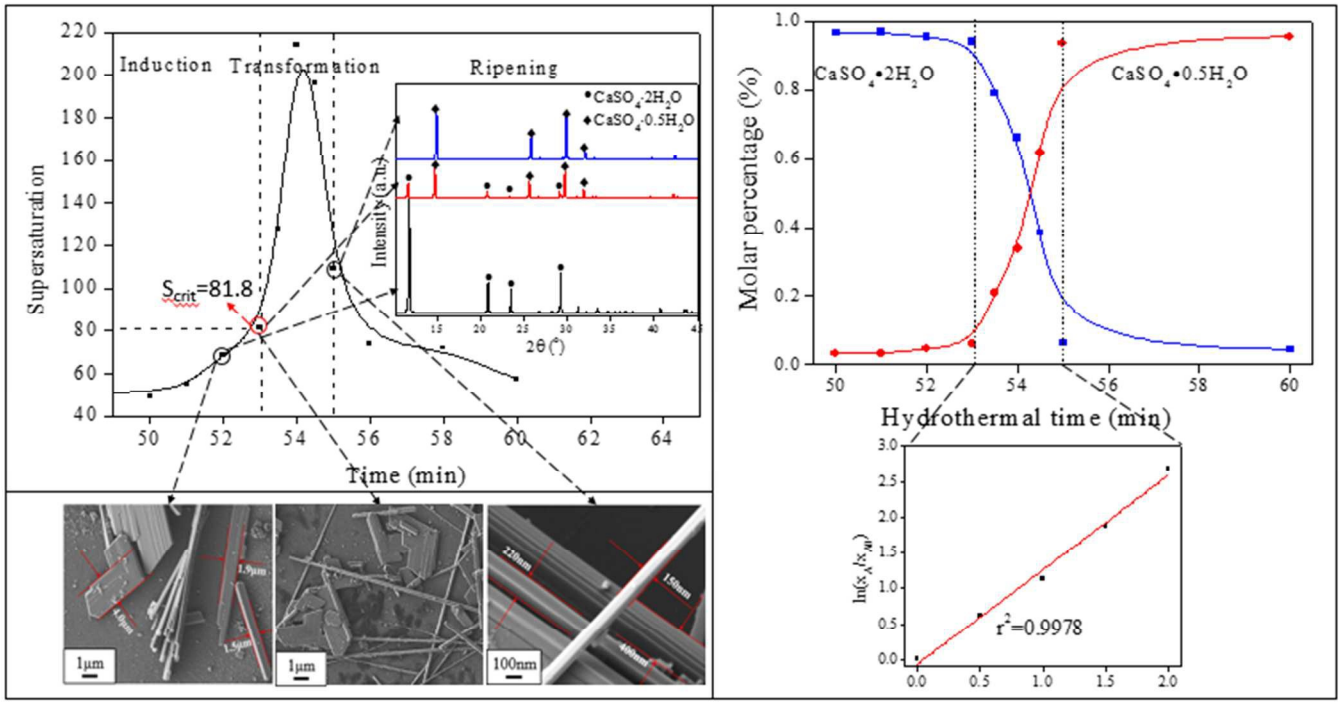

A supersaturation-induced fast transformation from $CaSO_4·2H_2O$ to α-$CaSO_4·0.5H_2O$ was observed and the process followed the dissolution-precipitation and homogeneous nucleation mechanism according to the classic nucleation theory.

AUTHOR CONTRIBUTIONS

Experiments and data analysis were conducted by S.C. Hou, J. Wang, and T.Y. Xue, the manuscript was written by S.C. Hou and revised by W.J. Zheng and L. Xiang. All authors have given approval to the final version of the manuscript.

ACKNOWLEDGEMENT

This work was supported by the National Science Foundation of China (No.51234003 and No.51174125) and National Hi-Tech Research and Development Program of China (863 Program, 2012AA061602).

REFERENCE

1. C. S. Cundy, P. A.Cox. *Chem. Rev.* **2003,** *103* (3), 663-702.
2. S.Yang, P. Y. Zavalij, M.S. Whittingham. *Electrochem. Commun.* **2001,** *3* (9), 505-508.
3. B.Liu, H. C. Zeng. *J. Am. Chem. Soc.* **2003,** *125* (15), 4430-4431.
4. L. E. Greene, M. Law, J. Goldberger, F. Kim, J. C. Johnson, Y. Zhang, R. J. Saykally, P. Yan. *Angew. Chem., Int. Ed.* **2003,** *42* (26), 3031-3034.
5. J. Wang, S. Hou, L. Zhang, J. Chen, L. Xiang. *CrystEngComm* **2014**.
6. L. Zhang, L. Yang, J. Wang, L. Xiang. *Int. J. Nanotechnol.* **2013,** *10* (1), 38-47.
7. J. Wang, S. Hou, H. Chen, L. Xiang. *J. Phys. Chem. C* **2014**.
8. S. Hou, L. Xian., *J. Nanomater.* **2013,** *2013*, 2.
9. M. Mo, J. Zeng, X. Liu, W. Yu, S. Zhang, Y. Qian. *Adv. Mater.* **2002,** *14* (22), 1658-1662.
10. C. M. Pina, M. Enders, A. Putni., *Chem. Geol.* **2000,** *168* (3), 195-210.
11. P. L. Nichols, M. Sun, C. Z. Ning. *ACS nano* **2011,** *5* (11), 8730-8738.
12. N. Kubota, M. Yokota, J. Mullin. *J. Cryst. Growth* **2000,** *212* (3), 480-488.
13. Z. Kožíšek; K. Sato; S. Ueno; P. Demo. *J. Phys. Chem.* **2011,** *134* (9), 094508.
14. P. Parimaladevi; K. Srinivasan. *Int. Dairy J.* **2014**.
15. K. Luo, C. Li, L. Xiang, H. Li, P. Ning. *Particuology* **2010,** *8* (3), 240-244.
16. K. Ishikawa. *Materials* **2010,** *3* (2), 1138-1155.
17. B. Wang, L. Yu, H. Wang, T. He. *Appl. Mech. Mater.* **2014**, *584-586*, 1618-1621.
18. X. Mao, X. Song, G. Lu, Y. Sun, Y. Xu, J. Yu. *Ind. Eng. Chem. Res.* **2014,** *53* (45), 17625-17635.
19. S. Nomura, K. Tsuru, S. Matsuya, I. Takahashi, I. Kunio. *Key Eng. Mater.* **2013,** *529*, 78-81.
20. S. Nomura, K. Tsuru, M. Maruta, S. Matsuya, I. Takahashi, K. Ishikawa. *Dent. Mater. J.* **2014,** *33* (2), 166-172.
21. S. Halevy, E. Korin, J. Gilron. *Ind. Eng. Chem. Res.* **2013,** *52* (41), 14647-14657.
22. HSC Chemistry 7.0, developed by Chemistry Software Ltd., Gateways, Kings Cross Lane, South Nutfield, Surrey, RH1 5NS, UK, 2013.
23. Mullin, J. W. *Crystallization*. Butterworth-Heinemann: 2001.